Preparation of MnO_2/Attapulgite Composites for adsorption of Ni(II)

Jianli Zhang, Yuan Yu and Weidong Liang*

School of Petrochemical Engineering, Lanzhou University of Technology, Lanzhou, GanSu, China.
Email: wdliangh@lut.edu.cn

Abstract. The emission of nickel ion has caused serious environmental pollution. Compared other techniques, adsorption has been used effectively to remove heavy metal ions. Attapulgite in Linze, a county of China, has low purity grade and poor adsorption performance. In order to improve the performance, a composite manganese dioxide/Attapulgite was prepared using simple stir. The effect of ATP-M on the adsorption researched of Ni^{2+} was investigated. The experimental results showed that adsorption capacity was related to the initial concentration pH and the dosage of adsorbents. ATP-M can reach max adsorption capacity to 63.69 mg/g under neutral conditions. The adsorption process was in line with pseudo-second-order kinetic model and the adsorption process was monolayer adsorption, which was more agreed with the Langmuir adsorption isotherm equation. Adsorption process was spontaneous with heat generation.

1. Introduction

In recent years, with the rapid development of industry, heavy metals have caused serious environmental pollution [1]. Due to the difficulty of remove, heavy metals could enter the human body through the digestive tract and pose a threat to human health [2]. Current methods for the treatment of heavy metals include physics, chemistry and biology [3]. Manganese oxide (MnO_2) is a kind of transition metal oxide, which has many advantages, such as large specific surface area, negative charge and many adsorption sites. Attapulgite(ATP) is a clay mineral with crystalline hydrated magnesia-aluminosilicate, which has the characteristics of specific surface area, ion exchange, adsorption capacity and so on. In this experiment, ATP-M composites were prepared by potassium permanganate and ethanol. The effects of the amount of adsorbent, the initial concentration, pH, and temperature on the adsorption of nickel ions were discussed.

2. Materials and Methods

2.1. Materials

The Attapulgite(ATP) from Gansu Linze, Hydrochloric acid (analytical purity, 37%), Potassium permanganate ($KMnO_4$), Ethanol, Deionized water.

2.2. Method

2.2.1. Preparation of ATP-M composites. ATP and sodium hexametaphosphate were dispersed at the ratio of 20:1, stirred for 12 h, dried at 50 °C, grinded and screened. Then, the dispersed ATP was transferred to a flake after using ultrasonic irradiation for 30min, and added a certain amount of $KMnO_4$ while keeping magnetic stirring for 1 h then 12 ml ethanol was added for 4h to make it come

into full contact. Finally, the composites were prepared by filtration, drying and grinding (named ATP-M).

2.2.2. Adsorption experiment. Firstly, the Ni^{2+} was determined by spectrophotometer and the standard curve was drawn. In a certain concentration of Ni^{2+} solution, adding a certain amount of ATP-M stirring for a period of time and standing for 2 minutes, the supernatant was filtered, and the concentration of Ni^{2+} was measured by spectrophotometer (V-1800, Shanghai, China). Each experiment was repeated twice to ensure the accuracy. The adsorbed amounts of nickel q_e, q_t and the removal rate R (%) were calculated.

$$qe = \frac{(C0-Ce)\times V}{M} \quad (1)$$

$$R(\%) = \frac{C0-Ce}{C0} \times 100 \quad (2)$$

Where q_e(mg/g) stands for equilibrium adsorption capacity of adsorbed Ni^{2+} ions, respectively. C_0 (mg/L) and C_e(mg/L) stands for the initial and equilibrium concentration. V(mL) stands for the volume of the Ni^{2+} solution, and m (g) stands for the amount of the adsorbent.

3. Result and Discussion

3.1. SEM Analysis.
Figure 1 shows the SEM of ATP and ATP-M. ATP rods can be watched in the SEM of ATP. ATP rods were relatively less and the aggregates were relatively serious, most of them were flake-like and plate-like [4], which indicated that there are other clay minerals such as montmorillonite, mica and feldspar. Figure b shows SEM of ATP-M. A mass of particles were observed on the surface of ATP-M, which indicated that part of the MnO_2 nano-particles were loaded on ATP.

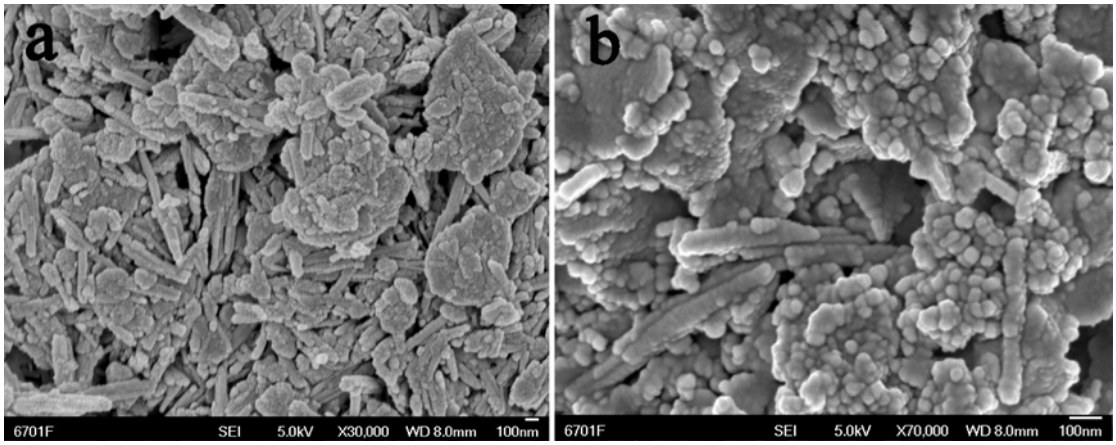

Figure 1. SEM images of (a)ATP and (b)ATP-M.

3.2. XRD Analysis.
Figure 2 shows the XRD diagram of ATP and ATP-M. The results show that ATP (2θ=8.27, 19.59, 27.91, 34.88) [5]. Muscovite(2θ=17.29, 29.89), chlorite(2θ=6.22, 12.27). quartz(2θ=20.75, 26.39, 50.02, 59.85). Feldspar(2θ=27.91). Montmorillonite(2θ=19.98, 35.06) (Standard Card: JCPDS NO.29-1498). For the ATP-M, the characteristic peak of MnO_2 were not very strong but there were characteristic peaks in 2θ=12.76 and 36.77 (110, 211) [6], which indicate that MnO_2 was successfully combined with ATP.

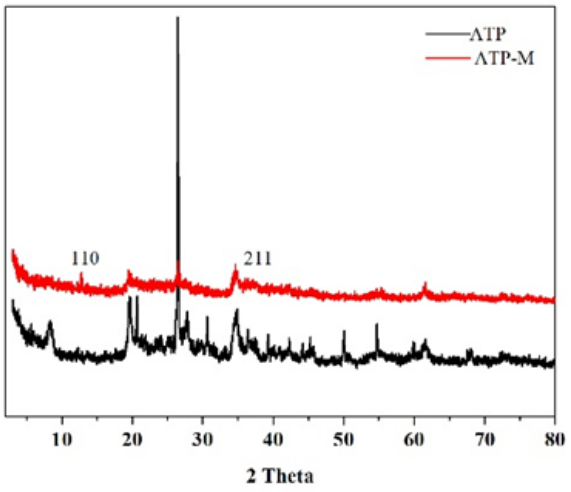

Figure 2. XRD of ATP and ATP-M.

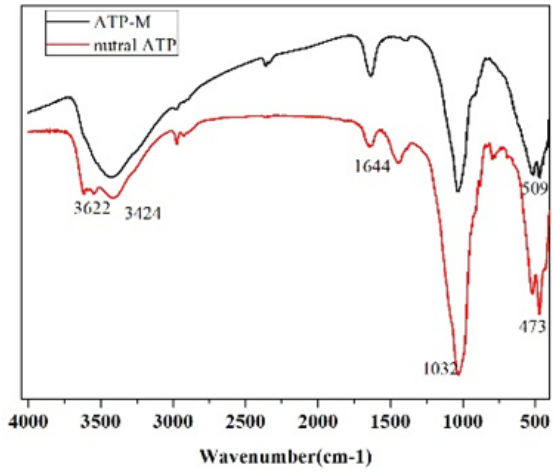

Figure 3. FTIR spectra of ATP and ATP-M.

3.3. FTIR Analysis.

Figure 3 shows the FT-IR of ATP and ATP-M. The band at 3622 cm^{-1} was caused by the stretching vibration of (Mg-OH, Al-OH, Fe-OH), the band at 3424 cm^{-1} was caused by the stretching vibration -OH of zeolite water and surface water [7].The weak band at 1644 cm^{-1} was caused by bending vibration H-O-H of coordination water and zeolite water. The poignant band at 1032 cm^{-1} was caused by stretching vibration of Si-O-Si. For the ATP-M, the characteristic peak appeared at 509 cm^{-1}, but it was not obvious. Through the comparison of literature and XRD analysis, this characteristic peak is the characteristic structure of Mn-O. The results show that MnO_2 was successfully combined with ATP.

4. Adsorption Isotherms and Parameters

4.1. Effect of Dosage of ATP-M, pH, Initial Concentration.

Figure 4 shows the effect of dosage of ATP-M, pH, initial concentration. From figure (4a), it can be seen that with the extension of the reaction time, the adsorption efficiency increases at first and then tends to equilibrium. The adsorption efficiency reached more than 90% in 60 min, which indicate that adsorption process was balanced in 60 min. The figure (4b) shows that the adsorption efficiency increases with the increase of the dosage of adsorbent. When the amount of adsorbent was 0.1g, the adsorption efficiency was more than 95%. However, the change of adsorption capacity was just opposite. These results might because the active site increases with the increase of the dosage of adsorbent. Figure (4c) shows that the removal rate increased with the increase of pH. When pH>8, Ni^{2+} forms precipitation, so the removal rate was more than 95%. Under the neutral condition, the removal rate reached about 90%, so the neutral condition was used in this experiment. Figure (4d) shows that the adsorption capacity increased with the increased of the C_0 and Adsorption capacity reached the maximum at 100 mg/L. However, the removal rate decreased. It might because of the number of ions increased with the increase of C_0, but 0.1 g ATP-M has reached the saturated and could not adsorb the excess ions, so the adsorption capacity decreased. Considering the comprehensive factors, 50 mg/L was used to be the initial concentration in this experiment.

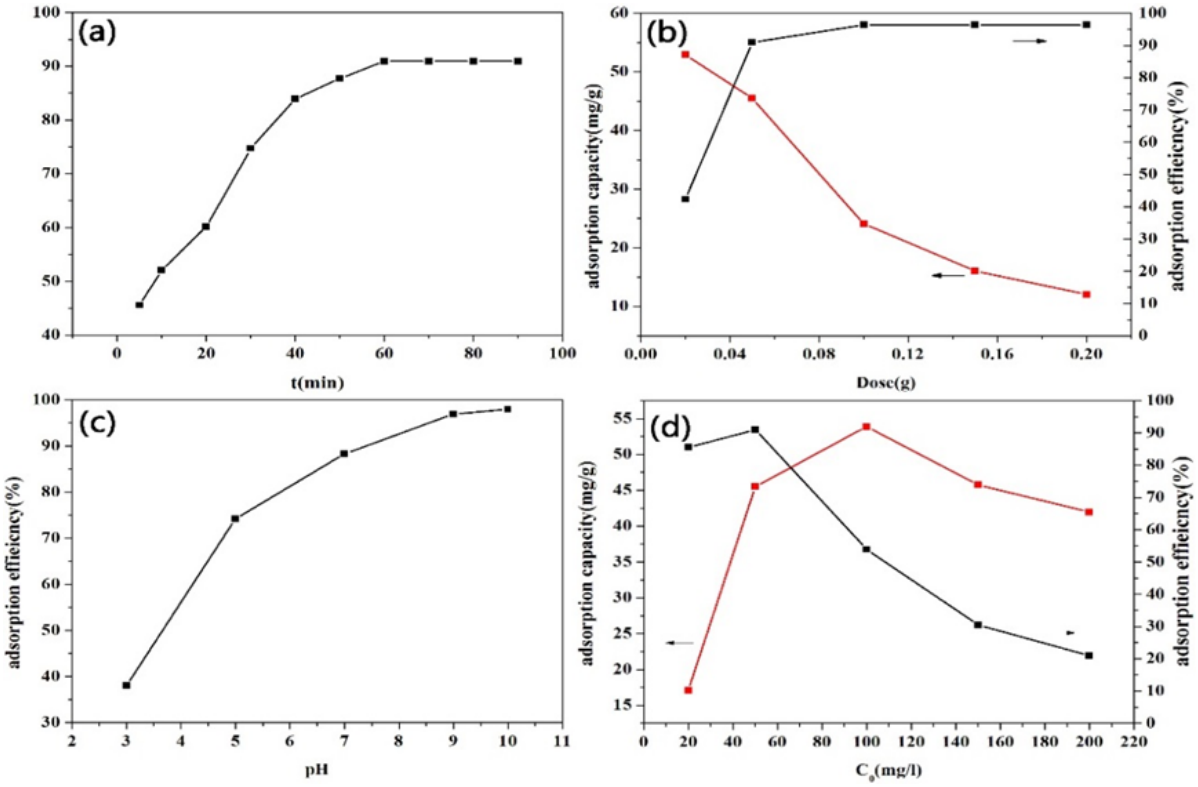

Figure 4. (a) Effect of contact time on Ni^{2+} adsorption (b) Effect of dosage of ATP-M on Ni^{2+} adsorption (c) Effect of pH on Ni^{2+} adsorption in solution (d) Effect of initial concentration of solution on Ni^{2+} adsorption.

4.2. Adsorption Kinetic Studies.

It can be seen from Figure 5 that concentrations of different of Ni^{2+} have the same kinetic curve. With the increase of time, the adsorption capacity increased at first and tended to adsorption equilibrium. Figure 6 shows the linear fitting of Ni^{2+} onto ATP-M, The pseudo-first order kinetic shown as (6a), The pseudo-second order kinetic shown as (6b), Results from linear Fitting of different dynamic equations shown in Table 1. It can be seen from Table 1 that the adsorption of Ni^{2+} by ATP-M accords with the pseudo-second order kinetics.

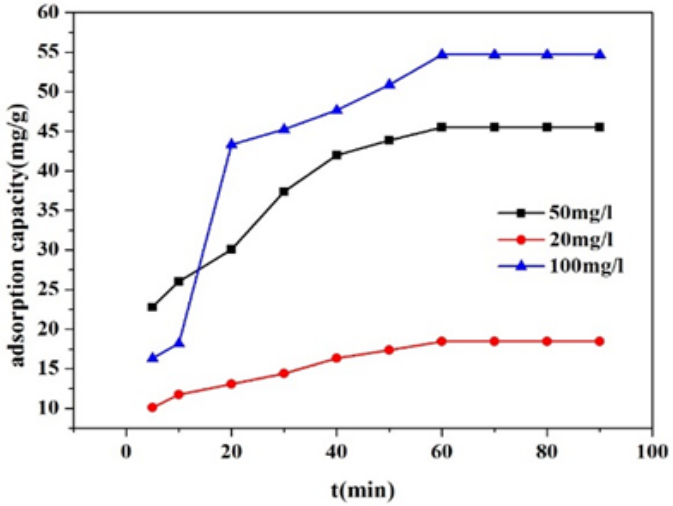

Figure 5. Adsorption kinetic curve of Ni^{2+} onto ATP-M

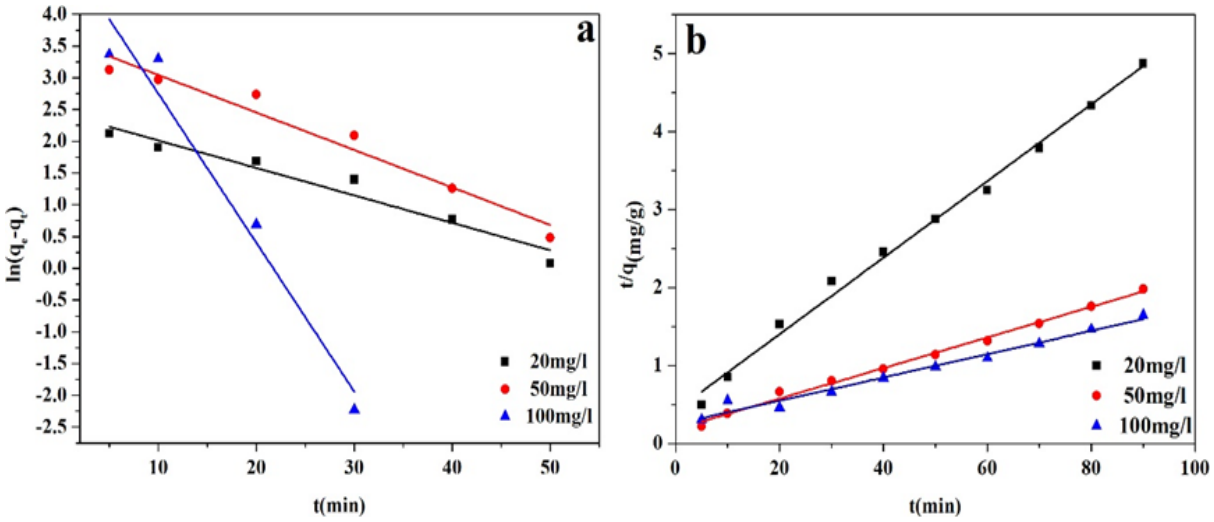

Figure 6. Linear fitting of Ni^{2+} onto ATP-M (a) The pseudo-first order kinetic (b) The pseudo-second-order kinetic.

Table 1. Results from linear Fitting of different dynamic equations.

C_0(mg/l)	pseudo-first order kinetic		pseudo-second order kinetic	
	k_1/min^{-1}	R^2	k_2/(g/mg/min)	R^2
20	0.100	0.941	0.00574	0.994
50	0.136	0.940	0.0021	0.994
100	0.540	0.945	0.0009	0.976

4.3. Thermodynamic Study.

Adsorption isotherm models for Ni^{2+}on ATP-M shown as Figure 7, Table 2 shows the two kinds of adsorption isotherm fitting parameters. The parameters of thermodynamic for the Ni^{2+} adsorption on ATP-M are shown in Table 3. According to the R^2, the adsorption process is more consistent with the Langmuir model.$\Delta G<0$ indicates the adsorption process was a spontaneous process. $\Delta H<0$ illustrates that the adsorption process was an exothermic reaction.

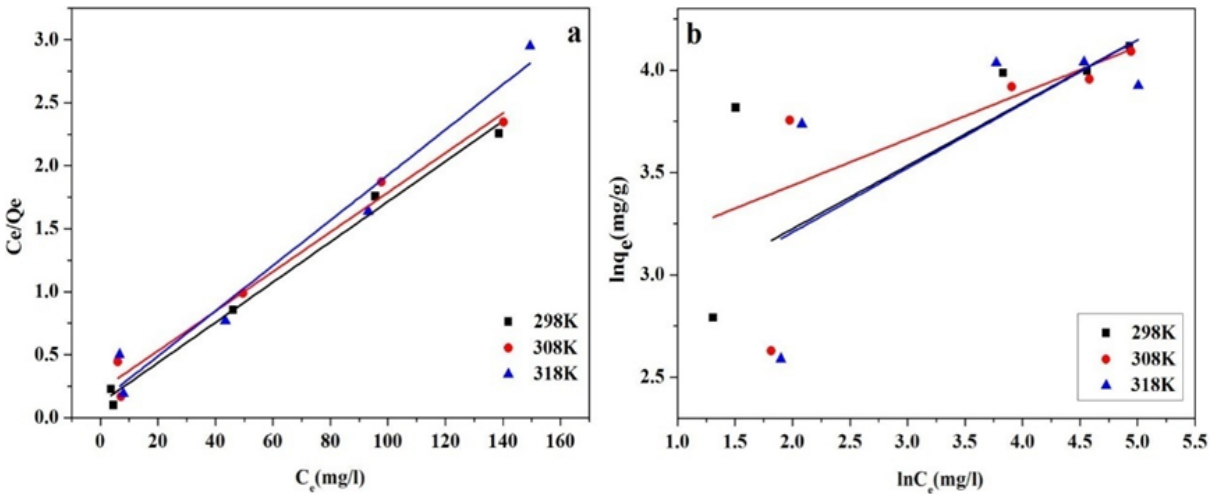

Figure 7. Adsorption isotherm models for Ni^{2+} on ATP-M.

Table 2. Two kinds of adsorption isotherm fitting parameters.

		Temperature(K)		
		298	308	318
Langumir	R^2	0.98915	0.9756	0.96333
	q_m	62.893	63.694	55.866
	d_L	0.1366	0.0726	0.1385
Freundlich	R^2	0.37507	0.43602	0.35961
	1/n	0.22576	0.30834	0.31332
	d_F	19.7964	13.5765	13.21893

Table 3. The parameters of thermodynamic for the Ni^{2+} adsorption on ATP-M.

T(K)	ΔG^0(KJ/mol)	ΔH^0(KJ/mol)	ΔS^0(J/mol/K)
298	-3.671		
308	-2.087	-31.37	-93.62
318	-1.827		

5. Conclusion

ATP-M is a cut-price and effective adsorbent for heavy metal ions. This simple prepared method makes the ATP of low purity plays a great application. The prepared composites have higher removal rate of Ni^{2+} and the adsorption process was spontaneous. The material of ATP-M could be used in treatment of heavy metal wastewater, which provides certain potential of application.

6. References

[1] Gupta S S , Bhattacharyya K G . Immobilization of Pb(II), Cd(II) and Ni(II) ions on kaolinite and montmorillonite surfaces from aqueous medium[J]. Journal of Environmental Management, 2008, 87(1):46-58.

[2] Jiang L, Liu L. Adsorption of Cobalt Ions and Nickel Ions from Wastewater by Modified Orange Peel[J]. Hubei Agricultural Sciences, 2016, 55(18):4675-4678.

[3] Saravanan R, Khan M M, Gupta V K, et al. ZnO/Ag/Mn_2O_3 nanocomposite for visible light-induced industrial textile effluent degradation, uric acid and ascorbic acid sensing and antimicrobial activity[J]. RSC advances, 2015, 5(44): 34645-34651.

[4] Zhang Z, Wang W, Tian G, et al. Solvothermal evolution of red palygorskite in dimethyl sulfoxide/water[J]. Applied Clay Science, 2018, 159: 16-24.

[5] Bradley W F. The structural scheme of attapulgite[J]. American Mineralogist: Journal of Earth and Planetary Materials, 1940, 25(6): 405-410.

[6] Huang C, Wang Y, Gong M, et al. α-MnO_2/Palygorskite composite as an effective catalyst for heterogeneous activation of peroxymonosulfate (PMS) for the degradation of Rhodamine B[J]. Separation and Purification Technology, 2020, 230: 115877.

[7] Li J J. Research of Flotation Process of Attapulgite Clay Mineral[D]. Beijing University of Chemical Technology, 2013.